BRIEF PAPER

Accurate Permittivity Estimation Method for 3-Dimensional Dielectric Object with FDTD-Based Waveform Correction

Ryunosuke SOUMA[†], **Shouhei KIDERA**[††a)], ***and*** **Tetsuo KIRIMOTO**[††], ***Members***

SUMMARY Ultra-wideband pulse radar exhibits high range resolution, and excellent capability in penetrating dielectric media. With that, it has great potential as an innovative non-destructive inspection technique for objects such as human body or concrete walls. For suitability in such applications, we have already proposed an accurate permittivity estimation method for a 2-dimensional dielectric object of arbitrarily shape and clear boundary. In this method, the propagation path estimation inside the dielectric object is calculated, based on the geometrical optics (GO) approximation, where the dielectric boundary points and its normal vectors are directly reproduced by the range point migration (RPM) method. In addition, to compensate for the estimation error incurred using the GO approximation, a waveform compensation scheme employing the finite-difference time domain (FDTD) method was incorporated, where an initial guess of the relative permittivity and dielectric boundary are employed for data regeneration. This study introduces the 3-dimensional extension of the above permittivity estimation method, aimed at practical uses, where only the transmissive data are effectively extracted, based on quantitative criteria that considers the spatial relationship between antenna locations and the dielectric object position. Results from a numerical simulation verify that our proposed method accomplishes accurate permittivity estimations even for 3-dimensional dielectric medium of wavelength size.

key words: *UWB pulse radar, permittivity estimation, non-destructive testing, non-invasive inspection, 3-D image reconstruction, range points migration (RPM) method*

1. Introduction

There are various demands for an innovative three-dimensional (3-D) imaging technique for objects embedded in dielectric media, aimed at highly reliable and non-invasive human body screening for medical purposes or the prevention monitoring of artificial structures to reduce a damage from natural catastrophes. As one of the most promising techniques that could satisfy those demands, electro-magnetic sensor systems using UWB (Ultra Wideband) signals come highly recommended, because it has sufficient range resolution and the desired dielectric penetrating capability.

To date, various kinds of internal imaging approaches for dielectric objects have been established. These are mainly classified into two schemes. One is the positioning or shape reconstruction scheme for objects buried in dielectric media using refocusing techniques such as space-time beamforming [1] or time-reversal focusing [2], aimed at the detection of tumors or unexploded buried landmines. However, these techniques are not necessarily suitable in identifying 3-D objects with clear boundaries, because these only provide a number of 2-dimensional (2-D) grayscale images, and require appropriate post-processing to reconstruct the accurate high-resolution 3-D image. The other scheme is mainly based on inverse scattering analysis using the domain integral equations [3]. Although this scheme directly reconstructs the spatial distribution of the dielectric constant even in inhomogeneous media, its accuracy or spatial resolution strongly depends on the assumed pixel size (directly related to the number of optimization variables). Also, to avoid sluggish convergence in multi-dimensional optimizations. there is a severe constraint on space discretization size. In contrast, the method in [4], aimed at through-the-wall applications, requires relatively smaller computational resources compared with methods described in [3] through use of the geometrical optics (GO) approximation. However, implementation of the method assumes the structures of the dielectric media are known and simple, such as rectangles.

As an effective solution for the above issue, we have already developed an innovative method, which simultaneously accomplishes accurate internal 2-D imaging and permittivity estimation [5]. This method employs the original RPM method [6] to correctly produce the dielectric boundary positions and their normal vectors. The actual time delay in propagating through the dielectric medium can then be accurately estimated from the recorded transmissive data. In particular, location and shape of an internal object are directly reconstructed by combining the exiting internal imaging method [8], which requires a correct dielectric constant for a surrounding dielectric object to accomplish highly accurate internal target reconstruction.

This study extends the existing permittivity estimation method [5] to the 3-D problem with an appropriate observation model. In this model, the transmissive and direct signals should be correctly discriminated without using *a priori* information of the dielectric object, while the effect of direct wave is negligible in the former 2-D model described in [5]. For this purpose, this method introduces quantitative criteria, which are calculated from the spatial relationship between an estimated dielectric shape by RPM and the transmitting and receiving antenna locations. Moreover, for dielectric medium of wavelength scale, the transmissive waveform differs from the transmitted waveform, and it reduces

Manuscript received July 25, 2013.
Manuscript revised October 23, 2013.

[†]The author is with Kyosan Electric Manufacturing Co., Ltd., Yokohama-shi, 230-0031 Japan.
[††]The authors are with the Graduate School of Informatics and Engineering, The University of Electro-Communications, Chofu-shi, 182-8585 Japan.
a) E-mail: kidera@ee.uec.ac.jp

DOI: 10.1587/transele.E97.C.123

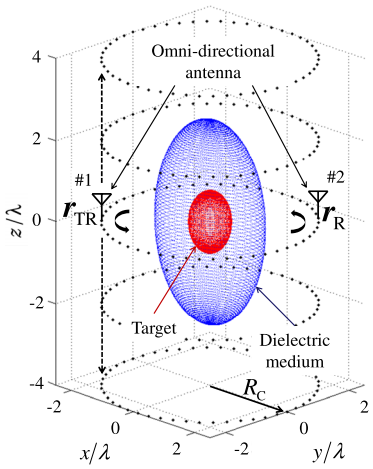

Fig. 1 System model in 3-D problem.

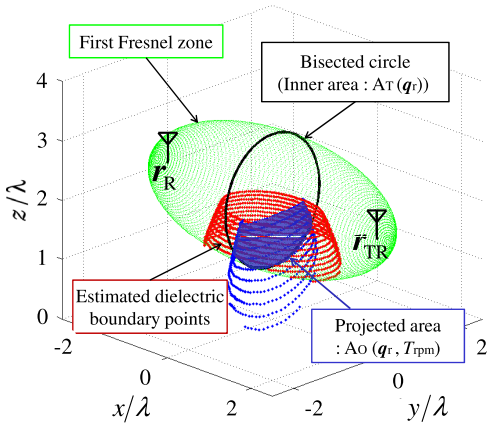

Fig. 2 Discrimination of direct and transmissive signal by the spatial relationship of the first Fresnel zone and the dielectric object position.

the accuracy of the time-delay measurement. Then, this extension also includes the waveform compensation process by regenerating the observation data using a finite-difference time domain (FDTD) method, similar to that given in [5]. The numerical-simulation-based validations show that our method provides accurate permittivity estimations, by taking a completely non-parametric approach even for 3-D targets of wavelength scale.

2. System Model

Figure 1 shows the system model. It assumes that target and dielectric medium have an arbitrary 3-D shape with clear boundaries. The dielectric object is a homogeneous, non-dispersive, and lossy medium. One omni-directional transmitting and receiving antenna is located at $\boldsymbol{r}_{\mathrm{TR}} = (X, Y, Z)$, the other antenna functioning only as a receiver is located at $\boldsymbol{r}_{\mathrm{R}} = (-X, -Y, Z)$. The pair of two antennae are scanned along a circle on the $z = Z$ plane, centered on the z axis with radius is $R_{\mathrm{c}} = \sqrt{X^2 + Y^2}$. A number of circular scannings on different z planes is performed, namely, those over the cylindrical surface with the z axis centering as shown in Fig. 1. A mono-cycle pulse is used as the transmitting signal, the center wavelength of which is defines as λ. $S_{\mathrm{TR}}(\boldsymbol{r}_{\mathrm{TR}}, R)$ and $S_{\mathrm{R}}(\boldsymbol{r}_{\mathrm{R}}, R)$ are defined as the output of the Wiener filter at antenna position $\boldsymbol{r}_{\mathrm{TR}}$ and $\boldsymbol{r}_{\mathrm{R}}$, respectively where $R = \mathrm{c}t/2$ is expressed by time t and the propagation speed of the radio wave c.

3. Proposed Permittivity Estimation Method

In [5], we have already discussed and verified that method [5] holds some advantages over existing approaches given in [3] or [4]. To avoid repetition, this letter forthwith introduces the 3-D extension of our previous method [5].

3.1 Dielectric Boundary Extraction by RPM

Similar to the 2-D approach, this method first employs the dielectric boundary points extracted by the RPM method [6], which achieves accurate imaging employing the observed range points defined as $\boldsymbol{q}_{\mathrm{DR},i} = (X_{\mathrm{DR},i}, Y_{\mathrm{DR},i}, Z_{\mathrm{DR},i}, R_{\mathrm{DR},i})$, $(i = 1, ..., N_{\mathrm{DR}})$ (DR denotes dielectric reflection). These points are extracted from the maxima of $S_{\mathrm{R}}(\boldsymbol{r}_{\mathrm{DR}}, R)$. Next, the RPM method directly converts these range points to the dielectric boundary points as $\boldsymbol{r}_i = (x_i, y_i, z_i), (i = 1, ..., N_{\mathrm{DR}})$, with the conversion being one-to-one. The normal vectors for all boundary points are directly calculated without the derivative operation as $\boldsymbol{e}_{\mathrm{n},i} = (X_{\mathrm{DR},i} - x_i, Y_{\mathrm{DR},i} - y_i, Z_{\mathrm{DR},i} - z_i)/R_{\mathrm{DR},i}$. In addition, to obtain target points and normal vectors on the dielectric boundary with a sufficiently small interval, the Envelope interpolation described in [7] and [8] is also introduced. Both boundary points and normal vectors are necessary for the proposed permittivity estimation scheme, particular in estimating the propagation path inside the dielectric medium.

3.2 Discrimination of Direct and Transmissive Signals

Here, it should be noted that the received signal $S_{\mathrm{R}}(\boldsymbol{r}_{\mathrm{R}}, R)$ includes both components of the direct and transmissive signals. The direct signal comprises a received component that propagates along a dielectric surface, called the creeping wave (which does not penetrate the dielectric medium). The transmissive signal is regarded as a received component that penetrates the dielectric medium that should be taken into account in the permittivity estimation. Depending on the particular spatial relationship among the transmitting, receiving antennas, and dielectric object position, $S_{\mathrm{R}}(\boldsymbol{r}_{\mathrm{R}}, R)$ might be dominated by the directly propagated component, and this signal should not be considered in the permittivity estimation processing. To address the above issue, this study introduces the discrimination scheme between the direct and transmissive signals, based on the quantitative criteria determined by the spatial relationship between the first Fresnel zone and the estimated dielectric boundary points, obtained by the RPM as previously described. This criteria qualitatively indicates that if the first Fresnel zone determined by the transmitting and receiving antenna locations is largely

occupied by the dielectric medium, the dominant component of the received signal in such an observation geometry should be classified as a transmissive signal. In this case, to establish quantitative criteria, the following index is introduced,

$$\zeta_{\mathrm{Fres}}(\boldsymbol{q}_{\mathrm{R}}) = \frac{A_{\mathrm{O}}(\boldsymbol{q}_{\mathrm{R}}, \mathcal{T}_{\mathrm{rpm}})}{A_{\mathrm{T}}(\boldsymbol{q}_{\mathrm{R}})}, \tag{1}$$

where $\boldsymbol{q}_{\mathrm{R}} = (X_{\mathrm{R}}, Y_{\mathrm{R}}, Z_{\mathrm{R}}, R_{\mathrm{R}})$ denotes the range point, which is extracted from the maxima of $S_{\mathrm{R}}(\boldsymbol{r}_{\mathrm{R}}, R)$ and $A_{\mathrm{T}}(\boldsymbol{q}_{\mathrm{R}})$ denotes the total surface of the circle on the bisected plane (called the bisected circle) by the line between the transmitting antenna and the receiving antenna, the region of which is determined by the first Fresnel zone. $A_{\mathrm{O}}(\boldsymbol{q}_{\mathrm{R}}, \mathcal{T}_{\mathrm{rpm}})$ denotes the projected region on the bisected circle, which is determined by the line of sight from each antenna location $(X_{\mathrm{TR}}, Y_{\mathrm{TR}}, Z_{\mathrm{TR}})$ or $(X_{\mathrm{R}}, Y_{\mathrm{R}}, Z_{\mathrm{R}})$ to the estimated dielectric boundary points denoted as $\mathcal{T}_{\mathrm{rpm}}$. If $\zeta_{\mathrm{Fres}}(\boldsymbol{q}_{\mathrm{R}}) > \zeta_{\mathrm{th}}$ holds, the $\boldsymbol{q}_{\mathrm{R}}$ is classified into the transmissive range point and is used in the permittivity estimation, which follows.

3.3 Permittivity Estimation with Transmissive Signal

To estimate the dielectric constant for an object, this method minimizes the difference between an observed and estimated propagation transmissive delay. Here, the relative permittivity is determined by

$$\epsilon_{\mathrm{t}}^{\mathrm{init}}\left(\boldsymbol{q}_{\mathrm{DT},i}\right) = \arg\min_{\epsilon_{\mathrm{t}}} \left| R\left(\epsilon_{\mathrm{t}} : X_{\mathrm{DT},i}, Y_{\mathrm{DT},i}, Z_{\mathrm{DT},i}\right) - R_{\mathrm{DT},i} \right|, \tag{2}$$

where $\boldsymbol{q}_{\mathrm{DT},i} = \left(X_{\mathrm{DT},i}, Y_{\mathrm{DT},i}, Z_{\mathrm{DT},i}, R_{\mathrm{DT},i}\right), (i = 1, ..., N_{\mathrm{DT}})$ denoting the transmissive range points (DT denotes dielectric transmission), which satisfy the criteria mentioned in Sect. 3.2 on the set of $\boldsymbol{q}_{\mathrm{R}}$. $R\left(\epsilon_{\mathrm{t}} : X_{\mathrm{DT},i}, Y_{\mathrm{DT},i}, Z_{\mathrm{DT},i}\right)$ is the estimated propagation delay using the RPM boundary points and normal vectors determined by the GO approximation. The procedure for the propagation path estimation is detailed in [5] for the 2-D model, but can be naturally extended to the 3-D model by an appropriate variable extension.

Using all the transmissive range points, the initial relative permittivity $\hat{\epsilon}_{\mathrm{t}}^{\mathrm{init}}$ is estimated next from

$$\hat{\epsilon}_{\mathrm{t}}^{\mathrm{init}} = \frac{\sum_{\boldsymbol{q}_{\mathrm{DT},i} \in Q} S_{\mathrm{R}}\left(\boldsymbol{q}_{\mathrm{DT},i}\right) \epsilon_{\mathrm{t}}^{\mathrm{init}}\left(\boldsymbol{q}_{\mathrm{DT},i}\right)}{\sum_{\boldsymbol{q}_{\mathrm{DT},i} \in Q} S_{\mathrm{R}}\left(\boldsymbol{q}_{\mathrm{DT},i}\right)}, \tag{3}$$

where $Q = \left\{ \boldsymbol{q}_{\mathrm{DT},i} \left| \epsilon_{\mathrm{t}}^{\mathrm{init}}\left(\boldsymbol{q}_{\mathrm{DT},i}\right) - \bar{\epsilon}_{\mathrm{t}}^{\mathrm{init}} \right| < \Delta\epsilon_{\mathrm{t}}^{\mathrm{init}} \right\}$, and $\bar{\epsilon}_{\mathrm{t}}^{\mathrm{init}}$ is the mode value calculated from the distribution of $\epsilon_{\mathrm{t}}^{\mathrm{init}}\left(\boldsymbol{q}_{\mathrm{DT},i}\right)$, $\Delta\epsilon_{\mathrm{t}}^{\mathrm{init}}$ is the threshold to eliminate outliers.

Note that the above procedure is basically derived from the GO approximation, where the frequency characteristic in transmissive phenomena is not taken into consideration. However, for a dielectric medium of wavelength scale, this frequency characteristic is not negligible and causes waveform deformation of the transmissive data, reducing the accuracy of the relative permittivity estimation, through inaccuracy in the range points.

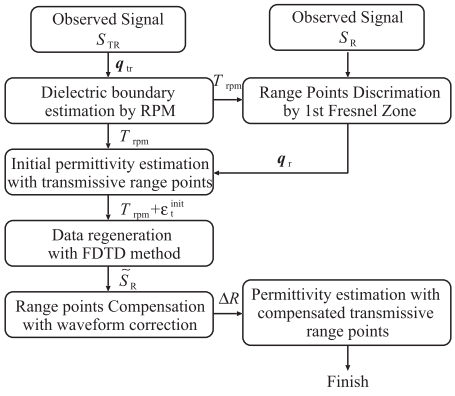

Fig. 3 Flowchart of the proposed method.

To compensate for the range errors caused by the waveform discrepancy between the transmitted and transmissive waveform, the FDTD data regeneration is applied using the initial guess of the permittivity and dielectric object. The detail of the approach are also the same in the 2-D model referred to in [5]. Specifically, we regenerate the transmissive data as $\tilde{S}_{\mathrm{R}}(\boldsymbol{r}_{\mathrm{DT}}, R)$ using the FDTD, where the dielectric boundary points as $\mathcal{T}_{\mathrm{rpm}}$ and the estimated relative permittivity as $\hat{\epsilon}_{\mathrm{t}}^{\mathrm{init}}$ are employed for FDTD data generation. Next, the range correction $\Delta R\left(\boldsymbol{q}_{\mathrm{DT},i}\right)$ at each range point $\boldsymbol{q}_{\mathrm{DT},i}$ is determined from the peak shift of the correlation function between the measured $S_{\mathrm{DT}}(\boldsymbol{r}_{\mathrm{DT}}, R)$ and the regenerated transmissive data $\tilde{S}_{\mathrm{DT}}(\boldsymbol{r}_{\mathrm{DT}}, R)$. The compensated relative permittivity $\epsilon_{\mathrm{t}}\left(\boldsymbol{q}_{\mathrm{DT},i}\right)$ for each range point is calculated as

$$\epsilon_{\mathrm{t}}\left(\boldsymbol{q}_{\mathrm{DT},i}\right) = \left\{ \sqrt{\hat{\epsilon}_{\mathrm{t}}^{\mathrm{init}}} + \frac{\Delta R\left(\boldsymbol{q}_{\mathrm{DT},i}\right)}{L_{\epsilon}\left(\boldsymbol{q}_{\mathrm{DT},i}\right)} \right\}^2, \tag{4}$$

where $L_{\epsilon}\left(\boldsymbol{q}_{\mathrm{DT},i}\right)$ is the estimated propagation distance in the dielectric medium for $\boldsymbol{q}_{\mathrm{DT},i}$ and $\hat{\epsilon}_{\mathrm{t}}^{\mathrm{init}}$ is the initial relative permittivity estimated by the weighted average of $\epsilon_{\mathrm{t}}^{\mathrm{init}}\left(\boldsymbol{q}_{\mathrm{DT},i}\right)$. Finally, the relative permittivity $\hat{\epsilon}_{\mathrm{t}}$ is determined through a weighted average similar to that given in Eq. (3). Note that, the estimation error for the permittivity estimation is mostly compensated for in the FDTD data regeneration only once, because the range errors are mainly caused by the frequency characteristic depending on the dielectric shape; the small error in the permittivity is negligible in regard to error compensation for each range point. Figure 3 shows a flowchart of the actual procedure for our proposed method.

4. Performance Evaluation of Numerical Simulation

This section presents performance validation of the proposed method, where the observation data are created by employing the FDTD method. Here, the dielectric object and the internal target shape are used as shown in Fig. 1. The boundary of the dielectric object is expressed as the ellipsoid $(x/1.5\lambda)^2 + (y/1.0\lambda)^2 + (z/2.5\lambda)^2 = 1$ holds, and that of the internal object is expressed as $(x/0.5\lambda)^2 + (y/0.5\lambda)^2 +$

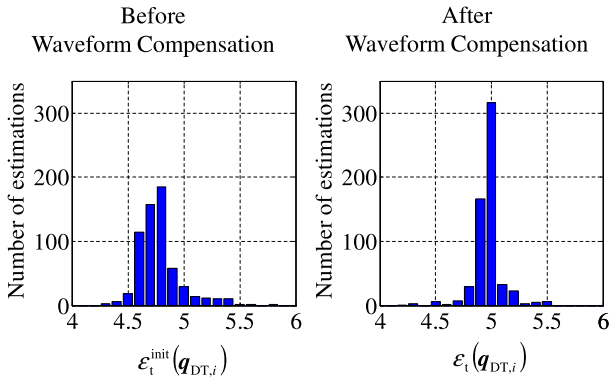

Fig. 4 Histograms of estimated relative permittivity before (left) and after (right) WC at S/N = 30 dB.

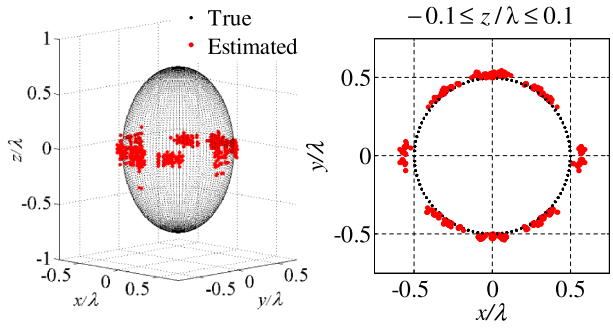

Fig. 5 Estimated internal image at S/N = 30 dB.

$(z/0.75\lambda)^2 = 1$ holds. The conductivity of the internal target is set to 1.0×10^7 S/m, and the conductivity and relative permittivity of the dielectric medium are set to 0.01 S/m and $\epsilon_{\mathrm{t}} = 5.0$, those values of which are typical for the case that a metallic pipe is buried in a concrete body. White Gaussian noise is added to $S_{\mathrm{TR}}(X, Y, Z, R)$ and $S_{\mathrm{R}}(X, Y, Z, R)$, where the signal-to-noise ratio (S/N) is defined as the ratio of the peak instantaneous signal power to the average noise power after applying the matched filter. $\boldsymbol{r}_{\mathrm{c}} = (0, 0)$ and $R_{\mathrm{c}} = 2.5\lambda$ are set, and the sample scanning for the antenna involves 51 (in the $x - y$ plane) and 40 (along z-axis) uniformly spaced points. $\Delta\epsilon_{\mathrm{t}}^{\mathrm{init}} = 0.5$ and $\zeta_{th} = 0.95$ are set in this case.

Figure 4 presents histograms of the estimated relative permittivity at S/N=30 dB, obtained at each range point before and after waveform compensation (abbreviated as WC). As shown in this figure, the mean and standard deviations of the estimated relative permittivity are considerably improved by the waveform correction of Eq. (4). The estimated relative permittivities before and after WC are $\hat{\epsilon}_{\mathrm{t}}^{\mathrm{init}} = 4.74$ (relative error: 5.2 %) and $\hat{\epsilon}_{\mathrm{t}} = 4.98$ (relative error: 0.4 %). These results demonstrate that the waveform correction approach is considerably effective. Figure 5 shows the internal target boundary points estimated using the method described in [8] and using the estimated permittivity with the proposed method. This figure visually verifies that the part of the internal estimation image is correctly reconstructed by using the accurately estimated dielectric constant. The asymmetric view of the obtained internal image is due to the shape of the dielectric object, which is ellipse at the cross section on the $x - y$ plane. Note also that there is an invisible area in the target boundary because the range points from this shadow area are not retrieved, owing to a distorted propagation path depending on dielectric boundary shape. However, this result shows that our proposed permittivity estimation is promising for accurate internal 3-D imaging without using the *a priori* dielectric constant or shape information. Finally, it should be noted that, in the typical nondestructive model, a shape of dielectric object and buried object would be cylindrical one, which is different from the model assumed in this letter. Since the cylindrical target model is almost equivalent to the 2-dimensional problem, its effectiveness can be analogized from the results obtained in the previous work [5]. Then, this letter assumes the ellipsoidal dielectric and buried objects to assess the proposed method in the fully 3-dimensional model, where the propagation path based on GO approximation should be curved along z axis.

5. Conclusion

Our study extended the former permittivity estimation method to a 3-D observation model, where suitable modifications were introduced, particularly in discriminating the transmissive and direct signals by establishing quantitative criteria. This method has a significant advantage over conventional techniques, and it is applicable to arbitrary unknown dielectric boundary shapes, and thus does not require any prior information such as dielectric constant or shape. In numerical simulations based on the FDTD method, our method reduced the relative errors in the relative permittivity estimation to less than 1%, even for the S/N = 30 dB data from an ellipsoidal dielectric medium. As a result, the internal image obtained employing the existing technique described in [8] provides a correct target shape even from noisy data.

References

[1] X. Li, E.J. Bond, B.D. Van Veen, and S.C. Hagness, "An overview of ultra-wideband microwave imaging via space-time beamforming for early-stage breast-cancer detection," IEEE Antennas Propag. Mag., vol.47, no.2, pp.19–34, Feb. 2005.
[2] P. Kosmas and C.M. Rappaport, "A matched-filter FDTD-based time reversal approach for microwave breast cancer detection," IEEE Trans. Antennas Propag., vol.54, no.4, pp.1257–1264, April 2006.
[3] A. Franchois and C. Pichot, "Microwave imaging-complex permittivity reconstruction with a Levenberg-Marquardt method," IEEE Trans. Antennas Propag., vol.45, no.2, pp.203–215, Feb. 1997.
[4] J. Ren, Y. Zhang, T. Jiang, and W. Chen, "Estimation of wall parameters from time-delay-only through-wall radar measurements," IEEE Trans. Antennas Propag., vol.59, no.11, pp.4268–4278, Nov. 2011.
[5] R. Souma, S. Kidera, and T. Kirimoto, "Accurate permittivity estimation method with iterative waveform correction for UWB internal imaging radar," IEICE Trans. Electron., vol.E96-C, no.5, pp.730–737, May 2013.
[6] S. Kidera, T. Sakamoto, and T. Sato, "Accurate UWB radar three-dimensional imaging algorithm for a complex boundary without range point connections," IEEE Trans. Geosci Remote Sens., vol.48, no.7,

pp.1993–2004, April 2010.
[7] S. Kidera, T. Sakamoto, and T. Sato, "High-resolution and real-time UWB radar imaging algorithm with direct waveform compensations," IEEE Trans. Geosci. Remote Sens., vol.46, no.11, pp.3503–3513, Nov. 2008.
[8] K. Akune, S. Kidera, and T. Kirimoto, "Accurate and nonparametric imaging algorithm for targets buried in dielectric medium for UWB radars," IEICE Trans. Electron., vol.E95-C, no.8, pp.1389–1398, Aug. 2012.